

Counterion effect on the formation of coordination polymer networks between AgNO₃ and L (2,2'-oxybis(ethane-2,1-diyl) diisonicotinate). Part 2.

Katharina M. Fromm^{a*}, Jorge L. Sague^{b*} and Markus Meuwly^c

^a University of Fribourg, Department of Chemistry, Ch. Du Musée 9, CH-1700, Fribourg, Switzerland.

Fax: (+41) 026 300 9738; Tel: (+41) 026 300 8732; E-mail: katharina.fromm@unifr.ch

^b University of Geneva – Sciences II, Department of inorganic, analytical and applied chemistry, , 30,

quai Ernest-Ansermet, CH-1211, Geneva 4, Switzerland. Fax: (+41) 022 374 6409; E-mail:

Jorge.sague@chiam.unige.ch

^c University of Basel, Department of Chemistry, Spitalgasse 51, CH-4056, Basel, Switzerland. Fax:

(+41) 061 267 3855; Tel: (+41) 061 267 3821; E-mail: markus.meuwly@unibas.ch

Supplementary data

A - I - DOSY EXPERIMENTS.....	2
A - II - FLUORESCENCE IN COMPOUND 2.....	2
A - III - PRINCIPAL HYDROGEN BOND INTERACTIONS IN COMPOUNDS 1 AND 3	4
A - IV - DISORDER IN COMPOUNDS 1-3. PROBLEMS FOUND IN THE REFINEMENT OF THE CRYSTAL STRUCTURE OF COMPOUND 2	5
A - V - TG/SDTA DATA FOR COMPOUNDS 1-3	5
A - VI - MAIN CRYSTALLOGRAPHIC SYMMETRY OPERATIONS FOR COMPOUNDS 1-3	6

A - I - DOSY experiments

The potential formation of a metallacycle in solution and the relationship between the concentration and the formation of some specific species was studied by NMR techniques such as DOSY. Experiments were performed in samples containing the ligand **L** and AgNO₃ in different concentrations. THF-d8 was used as solvent. The NMR tubes containing the samples for the DOSY-NMR measurements were prepared and sealed under argon atmosphere (Table 1).

Table 1. Hydrodynamic radii calculated based in DOSY-NMR experiments

	Solvent used, Temperature	DC (x 10 ⁻¹⁰ m ² /s)	Hydrodynamic radii (Å)
L	DMSO-d6,	3.23	3.55
L +AgNO ₃	298 K	2.46	4.66
L	THF-d8,	15.12	2.37
L +AgNO ₃	235 K	8.89	4.02

The radii calculated possess a ±5% error. Measure times from 15 to 20 ms.

Based on the diffusion coefficient (DC), the molar mass or hydrodynamic radii of species present in solution can be determined with a reasonable degree of error and consequently the molecular structure of these species derived. A limitation of this technique is that reliable diffusion coefficients can only be determined for well-resolved resonances. This can be problematic in the analysis of complex mixtures where signal overlapping can complicate the spectra.

The experimental diffusion coefficient (DC) obtained allows via the Einstein-Stokes equation $DC = k_B T / (6\pi\eta r_h)$ the calculation of the hydrodynamic radii. In this formula k_B is the Boltzmann constant, T the temperature in Kelvin, η the viscosity of the solvent employed and r_h the hydrodynamic radii (Table 1).

The DC of the solvent used are in the range reported in the literature (about 8-10 x 10⁻¹⁰ m²s⁻¹ for DMSO-d6 and THF-d8).

Differences above the limit of error were found for the sample containing the ligand **L** alone and the samples where the silver(I) complexes were formed. Differences in the mobility of the species were also found for the compounds when different concentrations were used.

The relation in the hydrodynamic radii ligand/complex in both cases implies the presence of oligomers ($-L-Ag^+-$)_n (n = 1,2) rather than polymeric species in solution in this range of concentration.

Although minimal, these differences may indicate the presence of a compound similar to the metallacycle in solution^{1, 2}. Some studies are being carried out in our group in order to get an insight into the process occurring in solution before the crystallization takes place.

A - II - Fluorescence in compound 2

Some silver complexes have been reported as being weakly fluorescent at room temperature, with some notable exceptions³⁻⁶. Recently Janiak *et al.* characterized a new silver(I) complex which exhibited fluorescence around 495 nm and related this phenomenon with weak Ag \cdots Ag contacts in silver complexes⁷. On irradiation at a wavelength value correspondent to its maximum absorption value, compound **2** shows some weak fluorescence (measurements were performed at 77 K) (Figure 1). In this compound inter- and intra-metallacycles Ag \cdots Ag interactions are present within the crystalline structure (Figure 2).

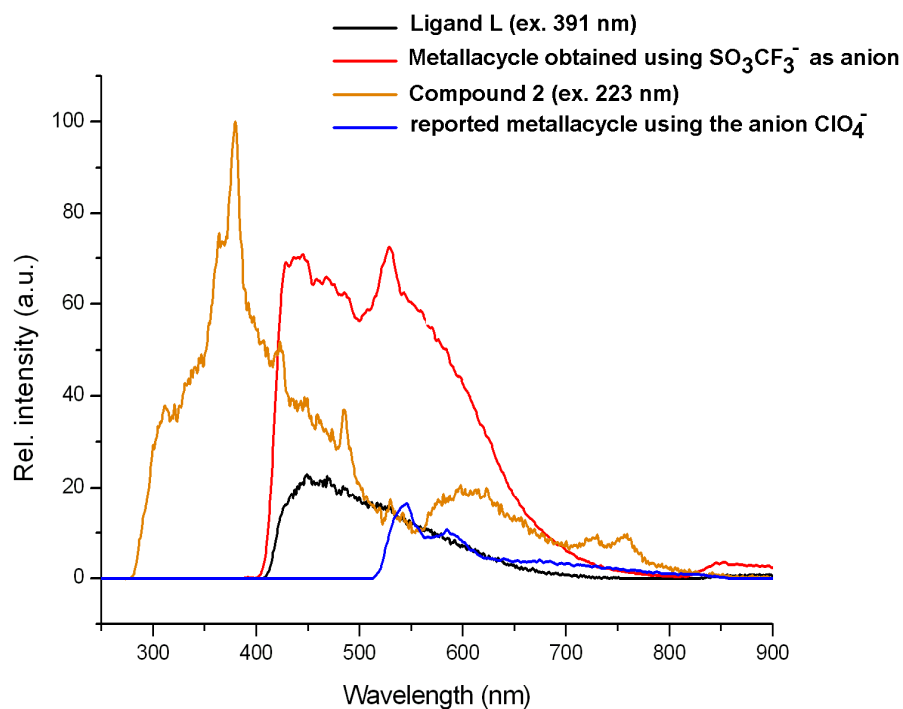


Fig. 1 Fluorescence measures in the solid state using crystals of compound **2** ($\{[Ag_2 \cdot L_2](NO_3)_2\}$, in orange colour). Blue and red colour represent the fluorescence for the crystals of the metallacycles $\{[Ag_2 \cdot L_2](ClO_4)_2\}$ and $\{[Ag_2 \cdot L_2](SO_3CF_3)_2\}$ respectively. The measure was performed at 77 K.

Despite usual assignments of weak fluorescence to LMCT processes, it is still quite difficult to establish a relationship between the results obtained here and the crystalline structure. Assigning the shape, intensity and location of peaks present in the curve for **2** to the presence of some type of $\{\cdots Ag \cdots Ag\}_n$ nanowires in the crystalline state is an attractive concept, but it clearly needs more experimental evidence.

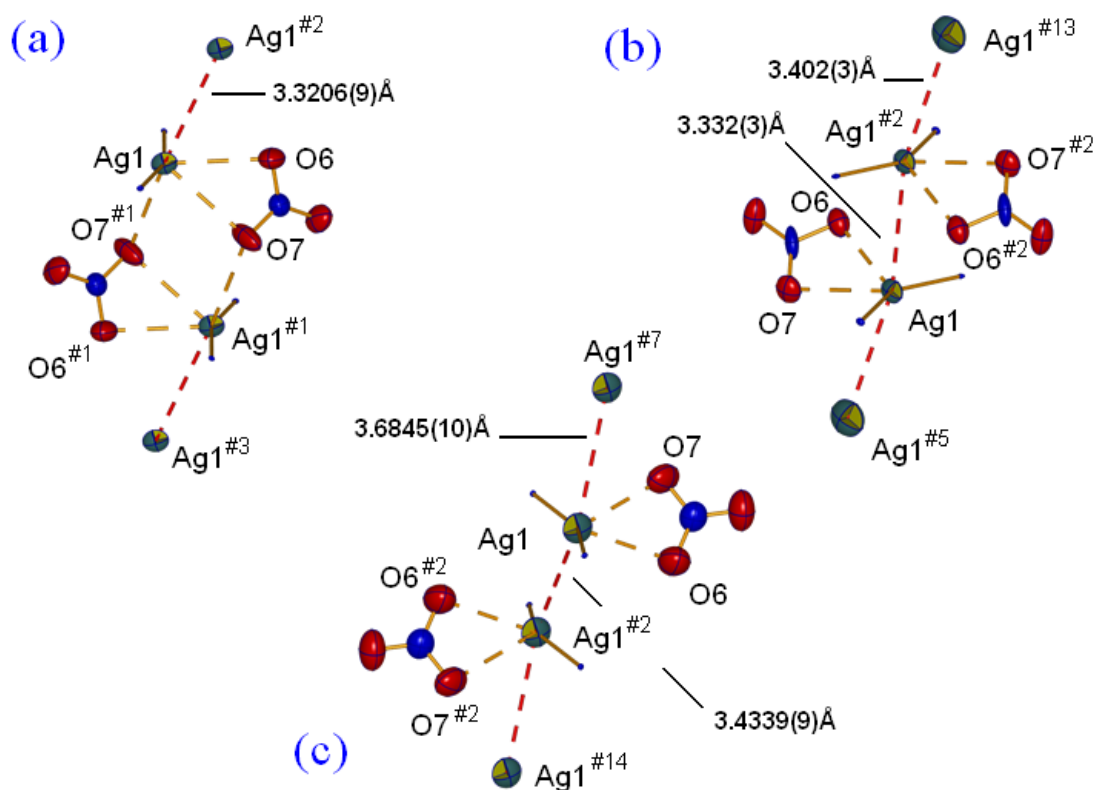


Fig. 2 Silver(I)···silver(I) interactions in compounds 1-3 (in red colour). The silver(I) atoms coordinated by NO_3^- counterions belong to the same metallacycle. (a) In compound 1, the $\text{Ag}\cdots\text{Ag}$ interactions are between different metallacycles; (b) both endo- and exo-metallacycles $\text{Ag}\cdots\text{Ag}$ interactions are present in compound 2; (c) in compound 3, these interactions are longer compared to those present in compound 2 (#1 -x, -y, -z, #2 -x, 1-y, -z, #3 x, -1+y, z, #5 -1-x, 1-y, -z, #7 1-x, 1-y, -z, #13 1+x, y, z, #14 -1+x, y, z).

A - III - Principal hydrogen bond interactions in compounds 1 and 3

Table 2. Hydrogen bond present in 1 [length (Å) and angle (°)]

D-H···Acceptor	d (D-H)	d (H···A)	d (D···A)	Angle D-H···A
O(9)-H(9E)···O(6)	0.81(6)	2.37(6)	3.072(5)	147(6)
O(9)-H(9E)···O(8)	0.81(6)	2.23(6)	2.984(6)	157(5)
O(9)-H(9F)···O(10)	0.82(6)	1.98(6)	2.788(6)	169(5)
O(10)-H(10E)···O(8) ^{#3}	0.94(9)	1.98(10)	2.842(6)	152(9)
O(10)-H(10E)···O(8) ^{#4}	0.71(7)	2.08(6)	2.760(5)	158(7)

Symmetry transformation used to generate equivalent atoms: #3 x, -1+y, z, #4 1/2-x, -1/2+y, 1/2-z.

Table 3. Hydrogen bond [length (Å) and angle (°)] present in complex 3

D-H···Acceptor	d (D-H)	d (H···A) Å	d (D···A) Å	Angle D-H···A
C(2)-H(2)···O(5) ^{#6}	0.93	2.37(0)	3.045(4)	130
C12-H12···O1 ^{#8}	0.93	2.43(0)	3.132(5)	132
C5-H5···O7 ^{#7}	0.93	2.51(0)	3.185(5)	129

A - IV - Disorder in compounds 1-3. Problems found in the refinement of the crystal structure of compound 2

In compounds 1-3 a positional disorder is present in the oxygen atom O3, located in the diethylene glycol chain. This disorder was mathematically modeled using the SHELX package in the three structures. The positions of the hydrogen atoms of the methylene carbon atoms (C8 and C9) adjacent to these oxygen atoms were modeled taken into account the disorder (for O3A the relate hydrogen atoms are H8A-B and H9A-B, and for O3B, H8C-D and H9C-D). In the particular case of compound 2 the R_I factor is rather high ($R_I=0.1237$ for 1360 and $R_I=0.2719$ for all 3804 data). There is not any remaining electronic density unassigned in this structure (the higher is $0.47 \text{ e}^-/\text{\AA}^3$). This high R_I factor value may be related to the absence of an appropriate correction of the diffraction data or the low amount of peaks collected during the measurement (due the poor diffraction of the crystal). The fact that these crystals were measured under room temperature may contribute as well to this value.

A - V - TG/SDTA data for compounds 1-3

To avoid ambiguities between compounds 2 and 3, TG/SDTA techniques can be used to unequivocally differentiate these compounds in the solid state (Figure 3 and Figure 4(a) and (b)).

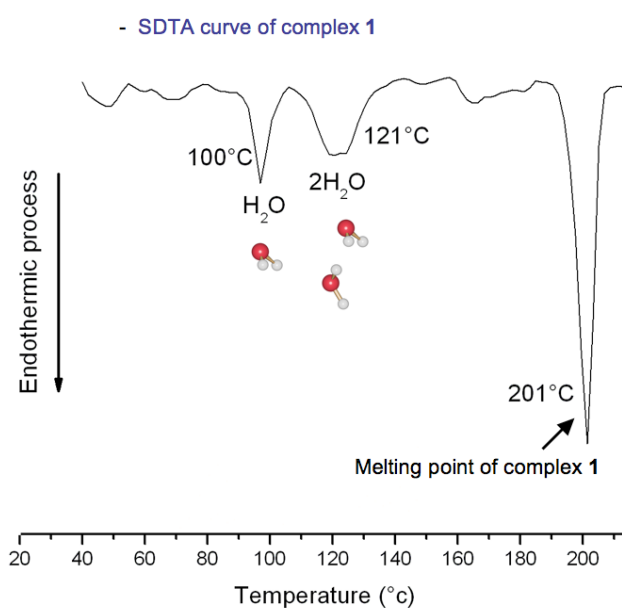


Fig. 3 SDTA curve for crystals of compound 1.

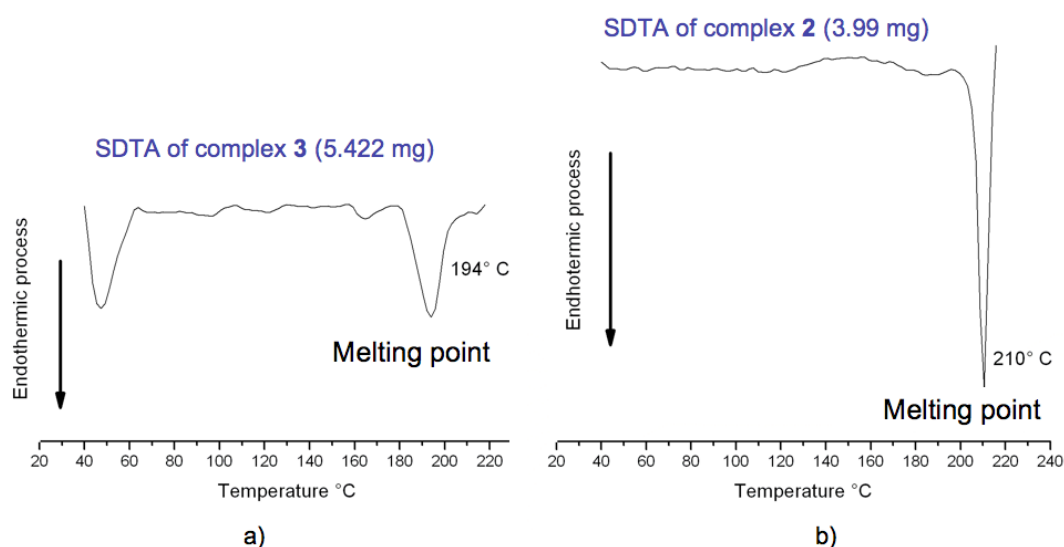


Fig. 4 SDTA curves for (a) compound 3 and (b) compound 2.

A - VI - Main crystallographic symmetry operations for compounds 1-3

- | | |
|---------------------------|------------------------------|
| #1 $-x, -y, -z$ | #9 $x, 1+y, z$ |
| #2 $-x, 1-y, -z$ | #10 $-1/2-x, -1/2+y, -1/2-z$ |
| #3 $x, -1+y, z$ | #11 $-1/2-x, 1/2+y, -1/2-z$ |
| #4 $1/2-x, -1/2+y, 1/2-z$ | #12 $x, y, -1+z$ |
| #5 $-1-x, 1-y, -z$ | #13 $1+x, y, z$ |
| #6 $-x, -y, 1-z$ | #14 $-1+x, y, z$ |
| #7 $1-x, 1-y, -z$ | |
| #8 $-x, 1-y, 1-z$ | |

1. S. Ahn, E.-H. Kim and C. Lee, *Bulletin of the Korean Chemical Society*, 2005, **26**, 331-333.
2. M. A. Jacobson, I. Keresztes and P. G. Williard, *Journal of the American Chemical Society*, 2005, **127**, 4965-4975.
3. Z. Liu, P. Liu, Y. Chen, J. Wang and M. Huang, *New Journal of Chemistry*, 2005, **29**, 474-478.
4. T. Wu, D. Li, X.-L. Feng and J.-W. Cai, *Inorganic Chemistry Communications*, 2003, **6**, 886-890.
5. S. Corni and J. Tomasi, *Journal of Chemical Physics*, 2003, **118**, 6481-6494.
6. S. Astilean and W. L. Barnes, *Applied Physics B: Lasers and Optics*, 2002, **75**, 591-594.
7. T. Dorn, M. Fromm Katharina and J. Christoph, *Australian Journal of Chemistry*, 2006, **59**, 22-25.
8. K. M. Fromm, J. L. S. Doimeadios and A. Y. Robin, *Chemical Communications (Cambridge, United Kingdom)*, 2005, 4548-4550.